ISBN: 978-3-95450-192-2 doi:10.18429/JACoW-IBIC2017-TUPWC04

# EXPERIMENTAL DAMPING SYSTEM WITH A FERRITE LOADED KICKER FOR THE ISIS PROTON SYNCHROTRON

A. Pertica*, D. W. Posthuma de Boer, ISIS, STFC, Rutherford Appleton Laboratory, Oxfordshire, OX11 0QX, UK

*Abstract*

The ISIS neutron and muon source, located in the UK, consists of a $H^-$ linear accelerator, a rapid cycling proton synchrotron and extraction lines towards two target stations. Transverse beam instabilities are one of the major factors limiting the intensity of the proton beam. In order to mitigate these instabilities an experimental damping system is being developed for the ISIS synchrotron. This system uses a split electrode beam position monitor (BPM) as a pickup and a ferrite loaded kicker as a damper. This kicker is ordinarily used to excite the beam with a fast rise time pulse for tune measurements. This paper describes the utilization of this device within a fast feedback system, using the continuous waveform provided by a split electrode BPM, which is processed by an FPGA board.

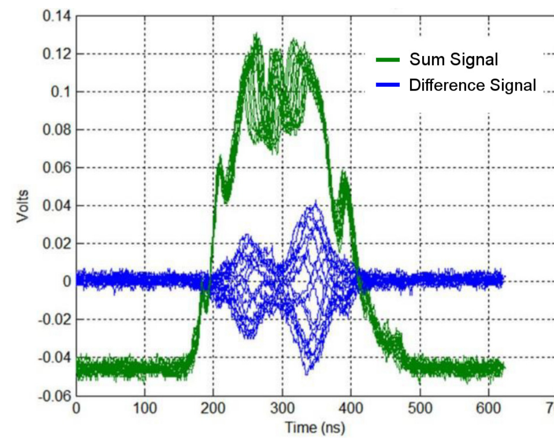


Figure 1: Sum and difference signals from a vertical BPM showing oscillations along a bunch [3].

## INTRODUCTION

### *The ISIS Synchrotron*

The ISIS synchrotron accelerates two proton bunches, with a total of $3 \times 10^{13}$ protons, from 70 MeV to 800 MeV at a repetition rate of 50 Hz, delivering a mean beam power of 0.2 MW to two tungsten targets. Protons are accelerated over 10 ms by first and second harmonic RF cavities, with a fundamental frequency sweep of 1.3 MHz to 3.1 MHz.

### *Instabilities at ISIS*

A coherent instability has been observed at ISIS, causing vertical emittance growth around 2 ms into the 10 ms acceleration cycle. BPM measurements taken over a number of turns have previously identified vertical oscillations along each bunch [1]; see Fig. 1. The sum signal in this figure shows the longitudinal profile of the bunch, while the difference signal provides an indication of the vertical position along the bunch. The oscillations shown in the difference signal are characteristic of a transverse $m = 1$ head-tail instability [2].

Operationally the head-tail instability is suppressed by ramping the vertical tune over the appropriate time interval. While this technique is effective, it is limited by losses as the vertical tune approaches the half-integer resonance [3].

### *The Feedback System*

A broadband, fast feedback system based on a stripline pickup & kicker has been designed to actively damp the effects of transverse instabilities and is currently being manufactured. Progress has been made on the feedback system itself by making use of the existing equipment in the ISIS synchrotron, specifically a split-plate BPM and a ferrite loaded kicker, the betatron exciter. The general set-up of the existing system is shown in Fig. 2.

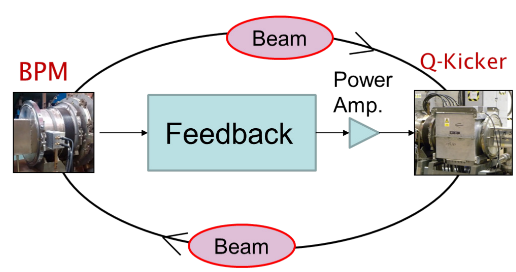


Figure 2: Set-up of the existing ISIS feedback system.

### *The Betatron Exciters*

The ISIS betatron exciters; or "Q-Kickers", are window frame ferrite loaded kickers in the synchrotron which are ordinarily used for measurements of beam tune; there is one such kicker for each transverse plane. They are formed of two high-voltage plates opposite to one another and surrounded by ferrite yokes. The plates are both terminated with a high-power 10 Ω load resistor. The layout of the Q-kicker is shown schematically in Fig. 3.

The Q-kickers are normally excited with 4 kV pulses of opposite polarity sent to each plate. The resulting electric and magnetic fields kick the beam for only a single turn. This kick produces betatron oscillations which are observed on BPMs around the ring.

* alex.pertica@stfc.ac.uk

ISBN: 978-3-95450-192-2 doi:10.18429/JACoW-IBIC2017-TUPWC04



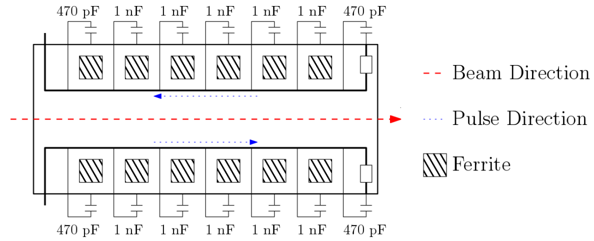

Figure 3: Internal layout of a Q-kicker, the direction of the two applied pulses is indicated as well as the beam direction.

### The Betatron Exciter as a Damper

As the Q-Kicker is typically used for tune measurements, it is often available during normal machine operation. For this reason it was decided to use it within a feedback system as a kicker to damp existing beam instabilities on the vertical plane. This has been achieved by driving the device with a linear power amplifier system at the end of a feedback chain, instead of a high voltage pulse generator.

## THE FAST FEEDBACK SYSTEM

### Kicker

In order to match the characteristic impedance of the Q-kicker, each of the two excitation plates are fed by a set of five 50 Ω URM67 coaxial cables from the electronics racks located 150 m away. As the Q-kickers are still needed as a betatron exciter no modifications have been made to the kicker itself. This allows the Q-kicker to be a damper or a betatron exciter by switching the inputs.

### Pick-up

A split-electrode BPM is used as a pick-up for the vertical plane. These monitors have a bandwidth that ranges from a few tens of kHz up to more than 50 MHz. The BPM located at the position with optimal betatron phase advance [4] (for a mean vertical tune of 3.8 around 2 ms) is used by another system. The next available BPM with the smallest phase advance error is located at 266° beta phase-advance upstream of the Q-kicker. Both electrode signals are amplified and sent through coaxial cables into the feedback electronics.

### Power Amplifiers

Each set of five coaxial cables is powered by a custom made *Eltac Ltd RA994 amplifier* providing five 50 Ω outputs. Both amplifiers are driven in anti-phase by the low level radio frequency (LLRF) stage. The amplifiers specifications are given in Table 1.

Table 1: Power Amplifier Specifications

| **Property** | **Value** |
|---|---|
| Frequency range | 50 kHz - 20 MHz |
| Phase linearity | 10° max variation |
| Gain | 51.5 dB nominal (±1 dB) |
| Rated Output Power | 20 W per output |

### Feedback Electronics

Figure 4 shows the block diagram for the feedback electronics. The LLRF stage receives the two electrode signals from the vertical BPM. One of these signals is feed through a programmable step attenuator, so the closed orbit offset can be subtracted from the differential signal at the 180° combiner. The resulting signal is then fed into the FPGA stage ADC. After being processed, it is fed back from the FPGA stage DAC into a programmable gain amplifier, a gating amplifier and a 180° splitter that provides the anti-phase signals for both power amplifiers.

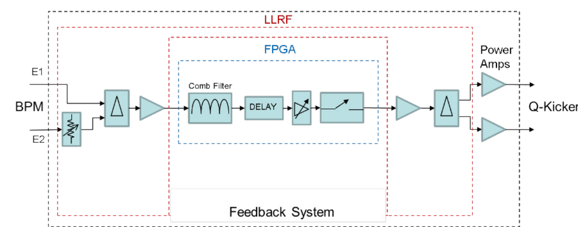

Figure 4: Block diagram of the feedback electronics.

The FPGA stage consists of a National Instruments NI-5781, 100 MS/s transceiver Flex-Rio front end module [5], backed by a PXIe-7962R Flex-Rio FPGA card. The first one samples the BPM differential signal to be processed by the FPGA and provides an analogue output for the LLRF stages. Both, the clock for the ADC/DAQ module and the FPGA processing stage are driven by a frequency synthesiser that multiplies the RF fundamental frequency by 30, tracking the bunch revolution frequency in order to simplify the filter implementation and delays adjustments. This block contains a comb filter to remove the revolution frequency and subsequent harmonics as well as the DC component.

Another stage produces a fixed delay for a calculated number of turns to apply the optimal kick (including the electronics and cable delays) and a dynamic delay that decreases as the revolution frequency ramps up. This stage also provides gating for the feedback signal – in order to apply the corrections only at a chosen time during the acceleration cycle. The gating and the look-up table managing block are driven by a 100 MHz clock in order to simplify the acceleration cycle synchronisation.

## INITIAL RESULTS

The initial tests aimed to check the suitability of the damping system for the existing head-tail motion in the synchrotron, around 2 ms after injection. First, measurements were taken with the feedback system disabled to record the existing instability. The system was then switched on with a gating time of 1.5 ms to 3.5 ms and optimised to produce the maximum damping. Afterwards, the signal fed to the power amplifiers was reversed in order to drive the beam and compare the effects. All graphs correspond to data sampled at 2.8 ms after injection where the instability effects were more noticeable. Beam parameters at 2.8 ms are listed in Table 2.

ISBN: 978-3-95450-192-2 doi:10.18429/JACoW-IBIC2017-TUPWC04

Table 2: Beam Parameters 2.8 ms after Injection

| **Property** | **Value** |
|---|---|
| Mean Vertical Tune | 3.7 |
| Revolution Frequency | 948 kHz |
| Kinetic Energy | 157 MeV |

Figure 5 shows the frequency spectrum with the feedback system disabled. The beam instability sidebands are evident around the fundamental RF frequency (1.886 MHz as there are two bunches in the ring).

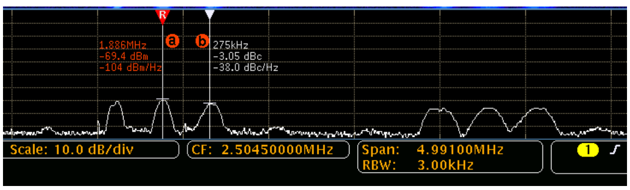


Figure 5: Frequency spectrum of the vertical BPM difference signal with the damping system disabled, showing the sidebands.

After switching the damping system on, the sidebands are attenuated by around 10 dB, as can be seen in Fig. 6

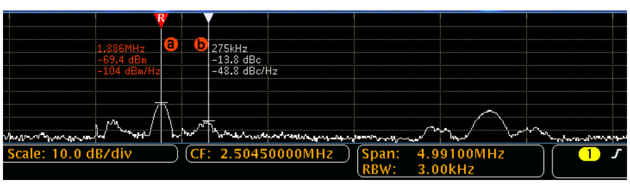


Figure 6: Frequency spectrum of the vertical BPM difference signal with the feedback system damping, showing the reduced sidebands.

By reversing the output signal polarity, in order to drive the beam, the initial sidebands were slightly increased, additional large sidebands were also observed; see Fig. 7.

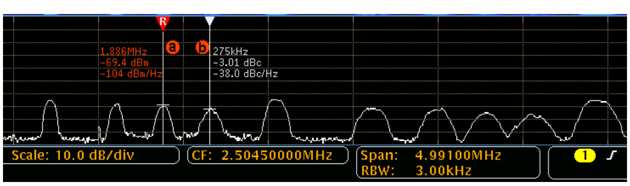


Figure 7: Frequency spectrum of the vertical BPM difference signal with the feedback system driving, showing additional sidebands.

The FFT waterfall graph in Fig. 8 shows the difference between the three scenarios. Each horizontal line in the waterfall graph corresponds to a set of FFT data acquired at a repetition rate of 1.6 Hz. The line at the bottom corresponds to the latest acquisition.

The top third corresponds to the damping system switched off, showing the sidebands clearly. The middle third corresponds to the damping system on, showing the sidebands reduced significantly. The bottom third shows the damping system driving the beam, with the sidebands slightly increased and the additional sidebands clearly visible.

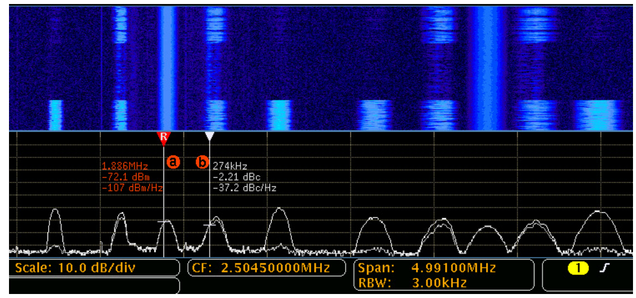


Figure 8: Waterfall plot demonstrating the effects of damping and driving with the feedback system.

Beam loss levels were compared between the three scenarios, integrating them during the time window between 1.5 ms and 2.5 ms. The reduction in beam loss with the damping system enabled was less than 5% and difficult to measure as the instability varied significantly between cycles. Further loss reduction may be achieved by tuning other beam parameters. The increase in loss was more evident while driving the beam.

## SYSTEM MODELLING

Modelling of the Q-Kicker has been performed using CST Microwave Studio® (MWS) [6]. The general structure of the model is shown in Fig. 9. The main features of the model are: the outer conductive casing, the ceramic vacuum vessel (green), the six ferrite window frames (blue), the plates connected via the feedthroughs, the lumped capacitors (blue, top and bottom) and the lumped resistors. The ferrite material was modelled as *Ferroxcube 4M2* with an electrical resistivity of $1 \times 10^5\ \Omega\,\mathrm{m}$, a constant relative permittivity of $\varepsilon = 10$ and a frequency dependent, complex relative permeability as specified in the material data sheet [7]. The beam apertures were modelled with open boundary conditions and the main body was grounded with space added above the electrical connections. The simulations were performed in the frequency domain as this allowed the permeability of the ferrite yokes to be interpolated rather than fit as is required in MWS time domain simulations.

### *Plate Coupling*

In order to test the validity of the model, initial simulations were performed which allowed comparison with experimental measurements. As the Q-kickers have been installed in the synchrotron only the 10 Ω plate input feedthroughs were available for measurement.

The coupling between the plates was measured with a Rohde & Schwarz ZVL vector network analyser (VNA). A resistive matching network was used to couple the VNA's 50 Ω ports to the 10 Ω feedthroughs, but was not included in the VNA calibration; the attenuation was added later. This setup was simulated by defining both of the 10 Ω feedthroughs

ISBN: 978-3-95450-192-2 doi:10.18429/JACoW-IBIC2017-TUPWC04



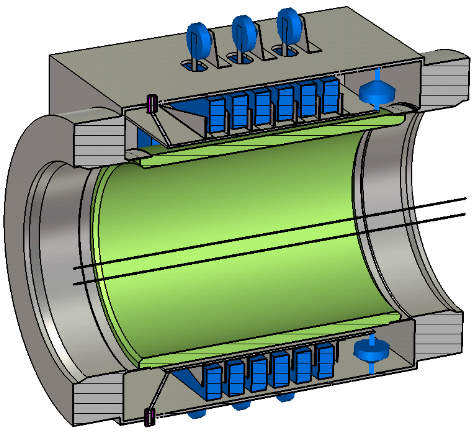

Figure 9: CST model of the Q-kicker with lumped elements and a two displaced wires.

as waveguide ports. The results of this simulation are shown in Fig. 10.

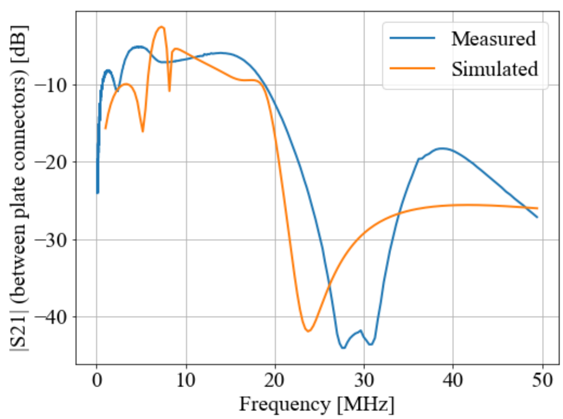


Figure 10: Simulated S-parameter magnitude of the coupling between opposing plates in the Q-kicker.

The measured results appear to match the simulated ones reasonably well between 6 MHz and 35 MHz. Some variation is expected due to mechanical and electrical imperfections. Below this frequency range however the simulated results consistently predict a smaller coupling between the plates than was measured; a difference of close to 7 dB at 1 MHz. Simulations with increased mesh density will be performed to investigate this observation.

### *Q-Kicker Frequency Response*

The frequency response of the Q-kicker was simulated by exciting a two wires, vertically displaced from the central axis; see Fig. 9, with opposite polarity using the multi-pin port feature of MWS. The two 0.5 mm radius, perfectly electrically conducting wires were displaced by ±1 cm from the central axis. The coupling to one plate connector was then obtained; see Fig. 11. The simulated response drops off significantly for lower frequencies. At 20 MHz the coupling

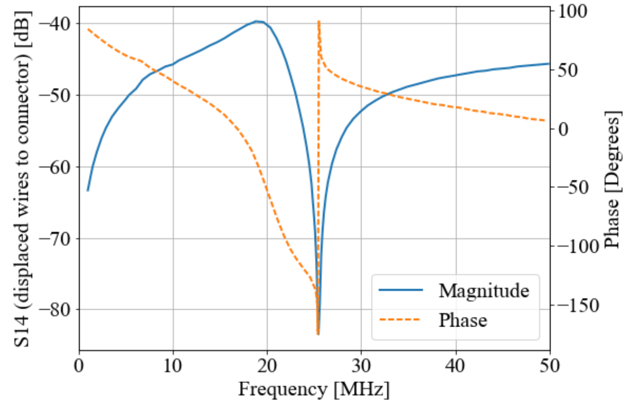


Figure 11: Simulated scattering parameters between two excited thin, displaced wires of opposite polarity and a 10 Ω feedthrough on one plate.

is predicted to be −40 dB, while at 1 MHz the coupling is less than −60 dB. Further simulation and beam-based measurements are required to verify whether this response is representative. Future simulations will excite the two plates simultaneously with opposite polarities, thus modelling real operation.

## CONCLUSION

Initial tests have shown a reduction of the instabilities around 2 ms with the feedback system on and in damping configuration, but was not consistent between pulses. More work can be done to improve the system by:

- Optimizing the parameters setup
- FPGA code improvements
- Power amplifier optimization
- Use a BPM in a more suitable location by duplicating electrodes signals

A simulation of the coupling between opposing plates in the Q-kicker has been compared with experimental measurements. The simulated and measured results share common features, with some appearing to have been shifted in frequency. Further work will be done to improve the model; this will initially look at improving the feedthrough geometry.

The simulated frequency response of the Q-kicker to two displaced wires showed a reduced response at lower frequencies, which could be investigated with beam-based measurements. Further simulations will be performed to verify this result.

## REFERENCES

[1] G. H. Rees, "Interpretation of the Higher Mode, Head-Tail Motion Observed on ISIS", *Part. Accel.*, vol 39, pp.159–167, 1992.

[2] F. J. Sacherer, "Transverse bunched-beam instabilities", CERN, Rep. CERN-PS-BR-76-21, Nov. 1976.

[3] R. Williamson, B. Jones and C. Warsop, "Development of Physics Models of the ISIS Head-Tail Instability", in *Proc. HB 16*, Malmö, Sweden, Jul. 2016.

ISBN: 978-3-95450-192-2 doi:10.18429/JACoW-IBIC2017-TUPWC04

[4] Z. Xie, "Transverse Beam Stability and Determination of Gain and Delay for Mixed-signal Transverse Feedback Dampers in Particle Accelerators", Ph.D thesis, University of Wisconsin-Madison, 2015.

[5] "NI-5781 Transceiver Adapter for FlexRIO", http://www.ni.com/en-gb/support/model.ni-5781.html,

[6] CST Microwave Studio®, www.cst.com, 2016.

[7] Ferroxcube, "4M2 Material Specification", http://www.ferroxcube.com/FerroxcubeCorporateReception/datasheet/4m2.pdf